Electronic Supplementary Material (ESI) for Chemical Communications.
This journal is © The Royal Society of Chemistry 2018

Supporting Information for

Heterobimetallic Single-Source Precursor Enables Layered Oxide Cathode for Sodium-Ion Battery

Maofan Li,[a] Kai Yang,[a] Jiajie Liu,[a] Xiaobing Hu,[b] Defei Kong,[a] Tongchao Liu,[a] Mingjian Zhang,*[ac] and Feng Pan*[a]

[a] School of Advanced Materials, Peking University, Peking University Shenzhen Graduate School, Shenzhen 518055, China.

[b] Condensed Matter Physics and Materials Science Department, Brookhaven National Laboratory, Upton, New York 11973, USA.

[c] Sustainable Energy Technologies Department, Brookhaven National Laboratory, Upton, New York 11973, USA.

∗Corresponding author: zhangmj@pkusz.edu.cn(M.Z.), panfeng@pkusz.edu.cn (F.P.)

Figure S8 TEM images of Na_xCoO_2 prepared by the single-source precursor method (a) and the traditional solid-state method (b).

Figure S9 CV curves for Na_xCoO_2 at a scan rate of 0.3 mV s^{-1}.

Figure S10 CV of $NaxCoO_2$ at different scan rates (0.3, 1, 5, 10 and 20 mVs^{-1}).

Figure S11 Nyquist plot of the cell measured at different temperatures before (a) and after (b) cycling.

3. Tables

Table S1 Elemental composition analysis by ICP-AES.

Table S2 Crystal Data and Structure Refinement Parameters for $NaCo(acac)_3$.

Table S3 Atomic Coordinates, Occupancies and Equivalent Isotropic Displacement Parameters for $NaCo(acac)_3$.

Table S4 Bond lengths (Å) and angles (°) for $NaCo(acac)_3$.

Table S5. XRD Refinement parameters of $NaCo(acac)_3$ and Na_xCoO_2.

Table S6. EIS parameters calculated from the Nyquist plot before and after cycling for Na_xCoO_2.

Table S7. The comparison of the rate capability for Na_xCoO_2 between the previous reports and this work.

1. Experimental Section

1.1 Preparation of single-source precursor

All chemicals were analytical grade and used as received without further purification.

(a) $C_5H_7NaO_2$: Sodium foils were added into acetylacetone in an argon-filled glove box. Leave it alone until the Sodium foils were completely exhausted to produce white powder $C_5H_7O_2Na$. After centrifugation, it was dried at 60 °C for 12 h in a vacuum oven.

(b) NaCo(acac)$_3$: $C_5H_7O_2Na$ (1.2808 g, 10.50 mmol) was dissolved in ethanol (40 mL), and $C_{10}H_{14}O_4Co$ (2.5715 g,10.00 mmol) was dissolved in ethanol (120 mL) under 55 °C with magnetic stirring. $C_5H_7O_2Na$ solution was slowly added dropwise to $C_{10}H_{14}O_4Co$ solution which keeps at 55 °C under magnetic stirring. Turn off heating after 1 hour with magnetic stirring continuing. After stirring for 5 hours, we can get the pink precipitate. It was filtered off, washed with ethanol several times (about 500 mL) and dried at 80 °C overnight in a vacuum oven. The synthesis process was carried out under nitrogen atmosphere. The complex is very stable in open air and soluble in strong polar solvent solvents (stronger than ethanol, such as methanol and water). The entire synthesis process was clearly shown in Figure S1.

1.2 Growth of single crystals

The powder of NaCo(acac)$_3$ was dissolved in a polarized solvent methanol with a small beaker. The small beaker with NaCo(acac)$_3$ solution was placed in a bigger beaker sealed with poor solvent ethanol. Then the entire setup was shelved in a cold closet of a refrigerator. After about 2 week, the orange prismatic single crystals were obtained in Figure S3.

1.3 Preparation of layered oxide cathode materials

For the single-source precursor method, the sample was obtained by calcining NaCo(acac)$_3$, in a Muffle furnace at 200 °C, 400 °C, 450 °C, 550 °C, 600 °C and 850 °C for 12 hours under air atmosphere.

As a reference, Na_xCoO_2 was also prepared by the traditional solid-state method. Na_2CO_3 and $CoCO_3$ was mixed in a Na/Co atomic ratio of 1:1. Then perform calcination at 850 °C for 12 hours under air atmosphere.

1.4 Materials characterizations

The X-ray diffraction (XRD) patterns of the single-source precursors and layered oxide materials were measured by a Bruker D8 Advance diffractometer using Cu-Kα radiation at room temperature. The scanning electron microscopy (SEM) images were measured by Zeiss SUPRA-55. Transmission electron microscopy (TEM) images were obtained using a FEI TecnaiG2 F30. Thermogravimetric analysis (TGA) data and differential scanning calorimetry (DSC) data of single-source precursors were collected on a TGA/DSC1 system from Mettle Toledo at a heating rate of 10 °C/min under air flow. The composition and distribution of chemical elements were observed by energy X-ray spectroscopy (EDX, Oxford X Max 20, 20 kV), and the ICP-AES analysis with HORIBA JY 2000-2. The diffraction data of $NaCo(acac)_3$ single crystals was collected by a Rigaku Saturn 944+ CCD diffractometer. The structures were solved by direct methods and refined by full-matrix least-squares method on F^2 with anisotropic thermal parameters for all atoms. All the calculations were performed with the Siemens SHELXTL version 5 package of crystallographic software. The parameters for data collection and the details of the structure refinement are presented in Table S2 and S3. Selected bond distances and angles are listed in Table S4. The tap density of Na_xCoO_2 is measured as 1.61 mg/cm^3 by a powder tap density tester (HY-100, Liaoning Bright Shine Machinery Co., Ltd).

1.5 Electrochemical measurements

The composite electrode was prepared by blending 80 wt% Na_xCoO_2 as the cathode active material, 10 wt% carbon black as the conductive additive, and 10 wt% poly(vinylidenefluoride) (PVdF) as the binder in N-methyl-2-pyrrolidone. The slurry was blade-coated onto aluminum foil and dried at 100 ℃ for 12 hours in a vacuum oven. Then electrode was cut into discs with diameter of 10 mm. The average mass loading of Na_xCoO_2 for each electrode is about 1 mg. Electrochemical tests were performed with CR2032 coin-type cells, which were finally assembled in an argon-filled glove box (Mikrouna Universal 2440/750) with water and oxygen content below 1 ppm. The pure Sodium foil was used as the anode. The glass microfiber filters (Whatman, GE Healthcare Life Science) was used as the separator. 1.0 M $NaClO_4$ in a mixture of EC : DEC = 1:1 (vol%) with 5 wt% FEC was used as the electrolyte. The cells were charged and discharged at different current densities in the galvanostatic mode. Before the electrochemical measurement, the prepared cells were shelved for 12 hours. Galvanostatic discharge/charge tests were performed using a NEWARE battery cycler in the voltage range of 2.0 - 4.0 V (*vs.* Na+/Na). The cyclic voltammetry (CV) and electrochemical impedance spectroscopy (EIS) test were performed on a CHI660 electrochemical workstation (Shanghai Chenhua Instrument Co., Ltd.). The EIS measurements were carried out in the frequency range of 1000 kHz to 0.01 Hz. The CV measurements were carried out with scan rates 0.3 mV S^{-1}. All the above data were collected at 25 °C.

2. Figures

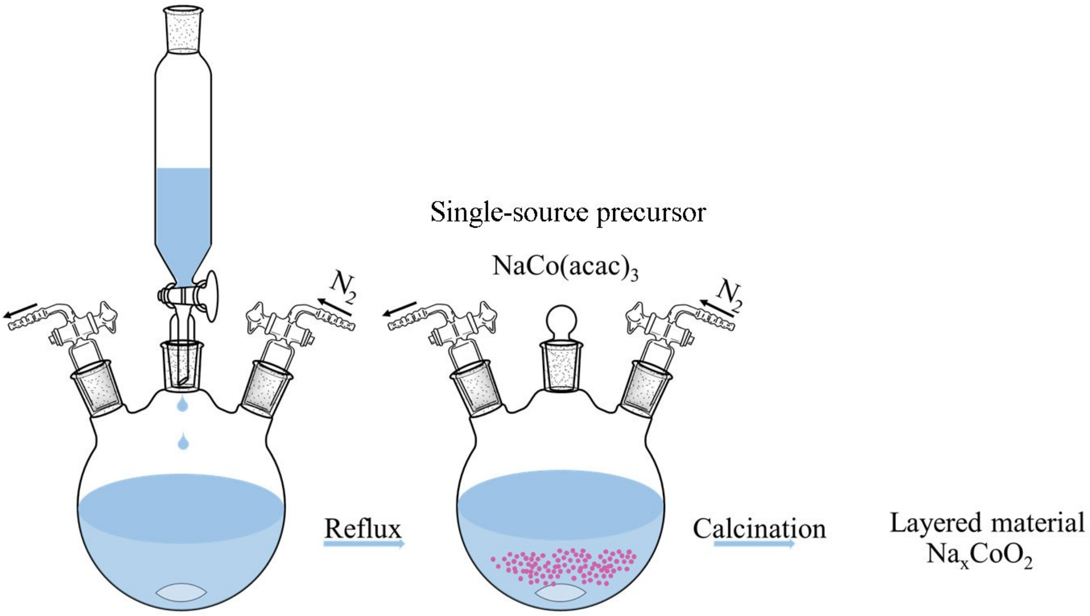

Figure S1 The schematic map showing the synthesis of layered Na_xCoO_2 by the single-source precursor method.

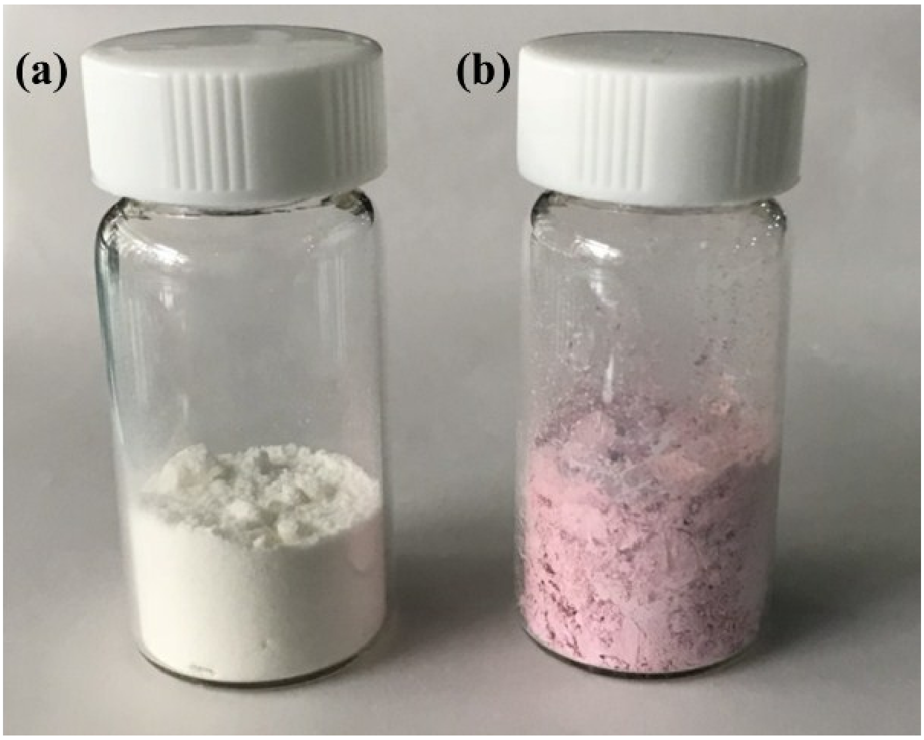

Figure S2 Photos of as-synthesized $C_5H_7O_2Na$ (a) and NaCo(acac)$_3$ (b).

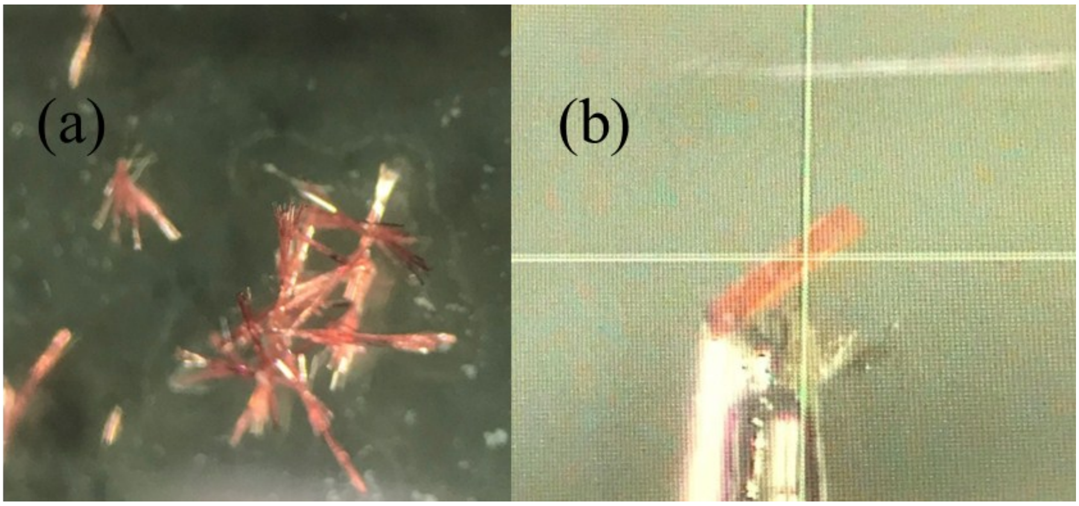

Figure S3 Photos of the NaCo(acac)$_3$ single crystals.

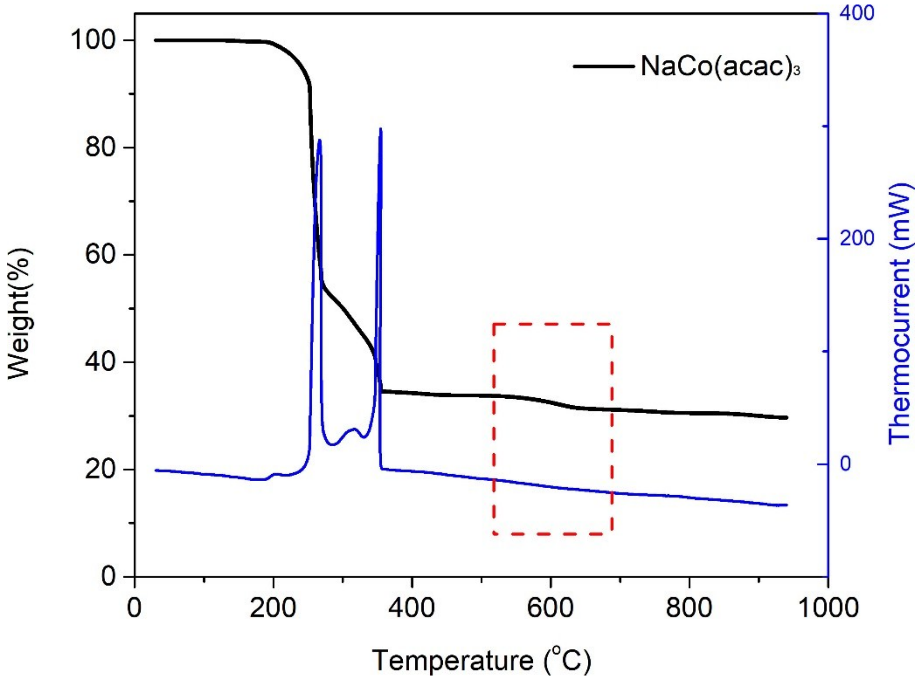

Figure S4 The TGA and DSC curves of NaCo(acac)$_3$.

To investigate the thermal stability of NaCo(acac)$_3$, thermogravimetric analysis (TGA) accompanied with differential scanning calorimetry (DSC) was performed (Figure S4, ESI†). Two obvious weight-loss steps were observed, including an abrupt weight loss behavior around 250 ℃ and a relatively slow weight loss behavior around 300 ℃. The experimental weight loss value 70.33% is basically consistent with its theoretical value 69.94% from precursor to layered oxide. Correspondingly, multiply exothermic peaks were observed in DSC curve, indicating a multiply-step thermal decomposition process. A small weight loss of about 2.44% was also observed at around 600 °C (marked with the red dashed rectangle). It should correspond to the majority of Na loss during the calcination, which is confirmed by the ICP-AES results (Table S1), and induces the formation of P3-Na_xCoO_2 (Figure S6).

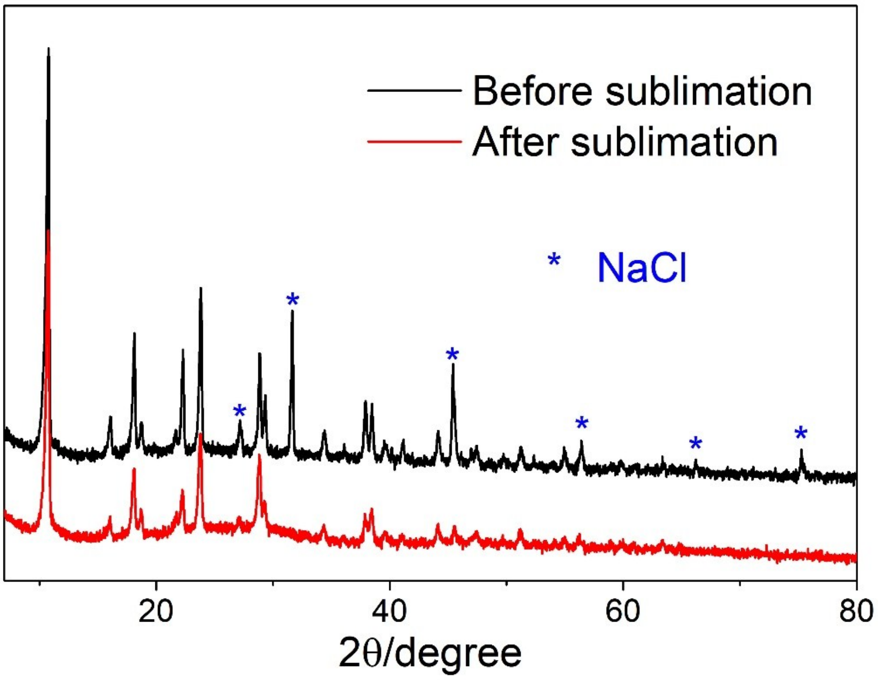

Figure S5 XRD patterns of $NaCo(acac)_3$ prepared using $CoCl_2$ as Co source before and after sublimation at 100 °C overnight.

According to the TGA data (Figure S4), we performed the sublimation experiments for $NaCo(acac)_3$ synthesized using $CoCl_2$ as Co source at 100 °C before it decomposes. The purity of the products has been checked by the XRD experiments before and after sublimation as below. It is clear, after heating at 100 °C overnight, pure $NaCo(acac)_3$ was obtained by removing the NaCl impurity.

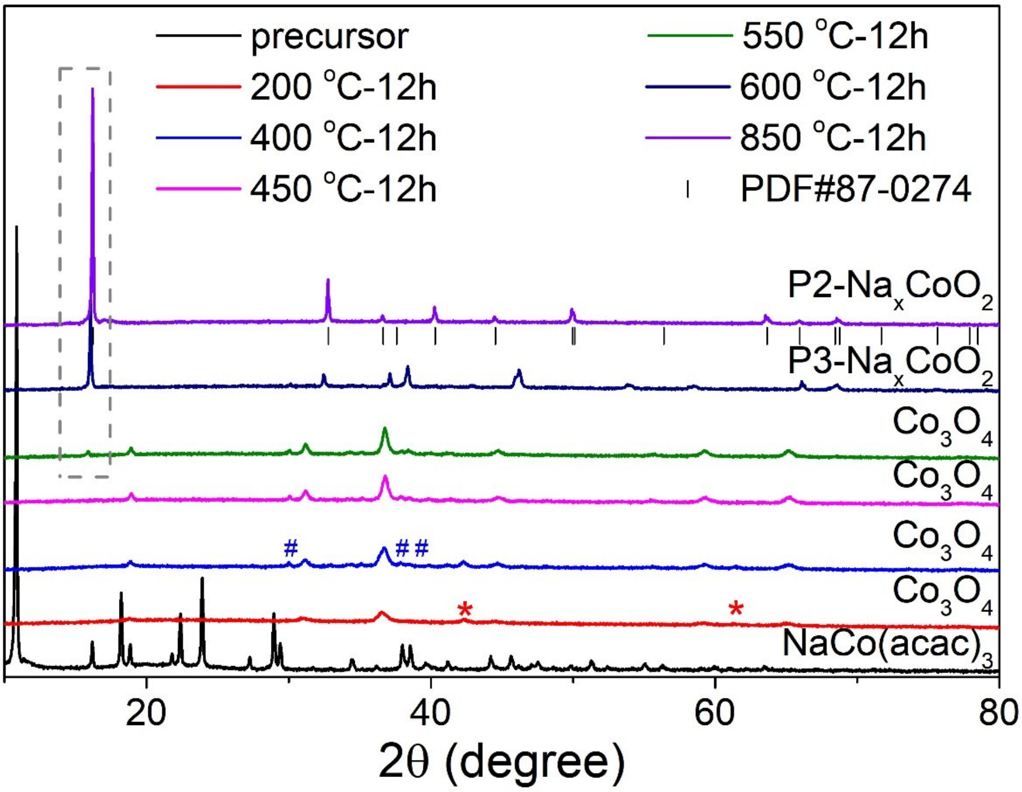

Figure S6 The XRD patterns of NaCo(acac)$_3$ calcined at different temperatures for 12 hours. The red asterisks and blue pounds were used to mark some impurity, which might be some kind of Na source, but could not be identified (not NaOH, Na_2CO_3, $NaHCO_3$, Na_2O or Na_2O_2).

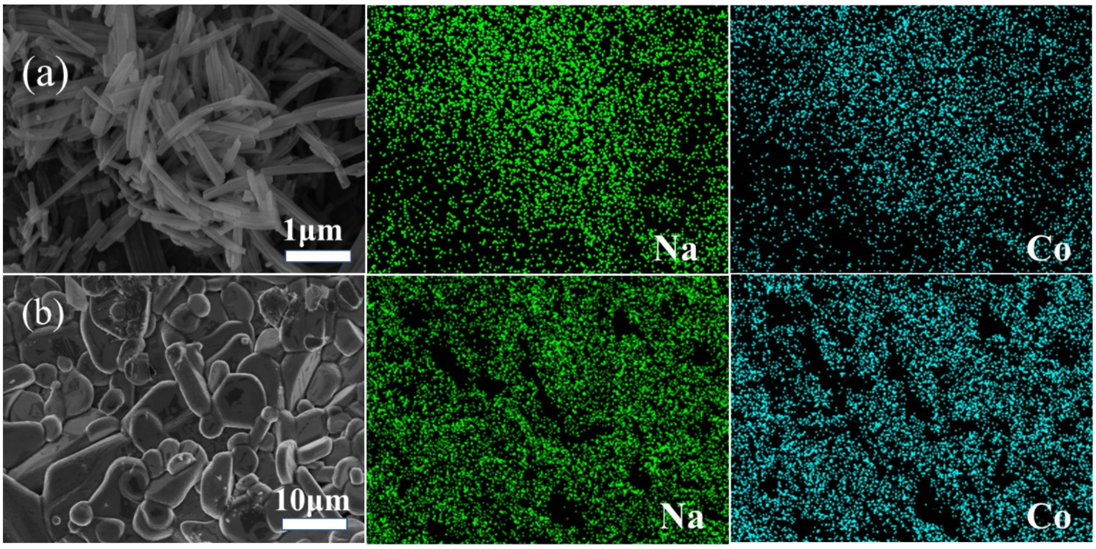

Figure S7 SEM elemental mappings of NaCo(acac)$_3$ (a) and Na$_x$CoO$_2$ (b).

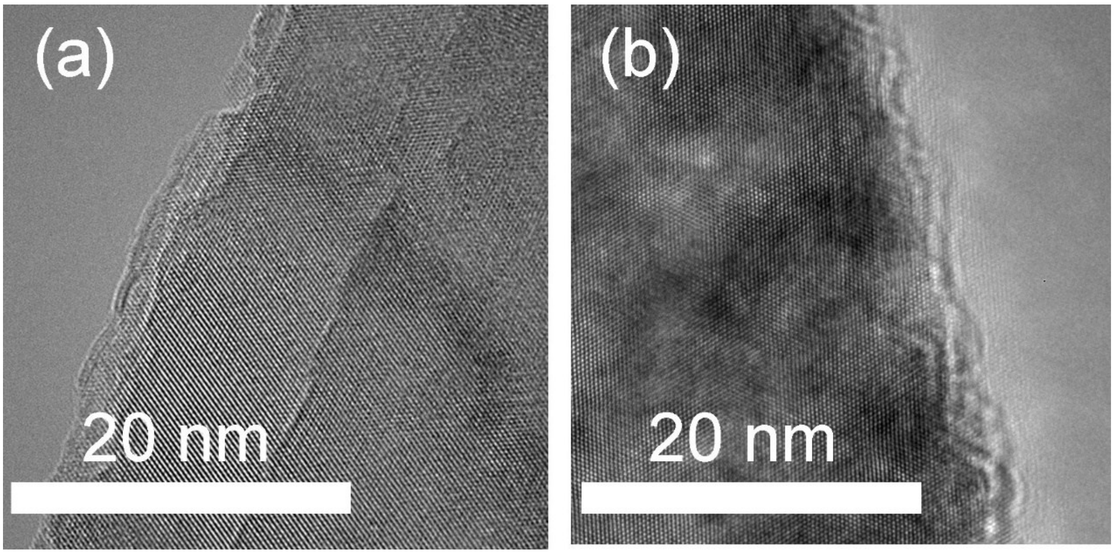

Figure S8 TEM images of Na_xCoO_2 prepared by the single-source precursor method (a) and the traditional solid-state method (b). It is obvious that the former delivered a much cleaner surface.

The TEM images above clearly demonstrate that, the sample obtained by the single-source method has a much cleaner surface than the sample obtained by the traditional solid-state method. It could be responsible for the little difference of the voltage profiles between the 1st cycle and the subsequent cycles in Figure 4, which always results from the surficial residues, such as NaOH, $NaHCO_3$, Na_2CO_3 and etc., at the particle surface.

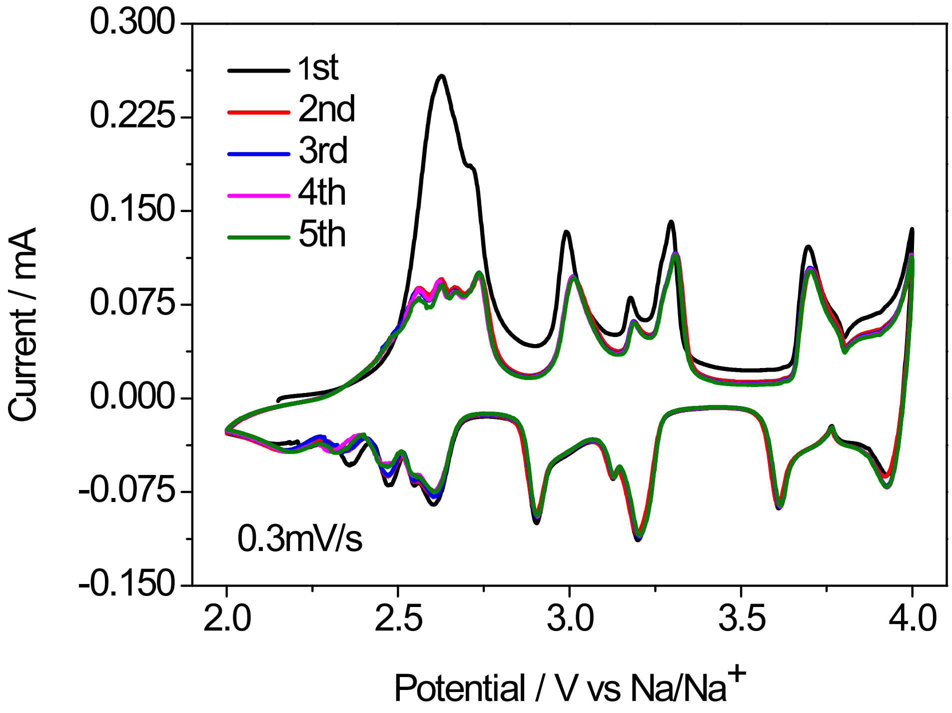

Figure S9 CV for Na_xCoO_2 at a scan rate of 0.3mV s^{-1}.

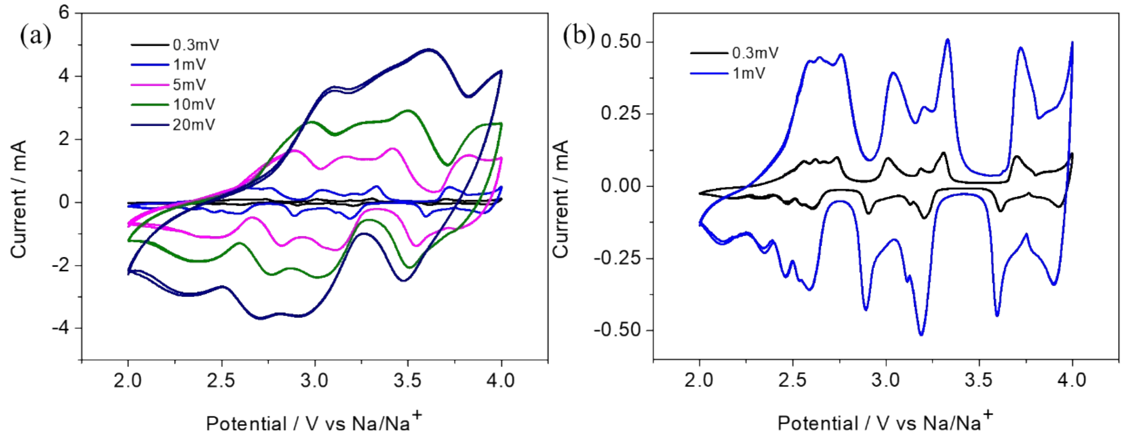

Figure S10 (a) CV curves of Na_xCoO_2 at different scan rates (0.3, 1, 5, 10 and 20 mV s^{-1}); (b) the enlarged CV curves at scan rates of 0.3 and 1 mV s^{-1}.

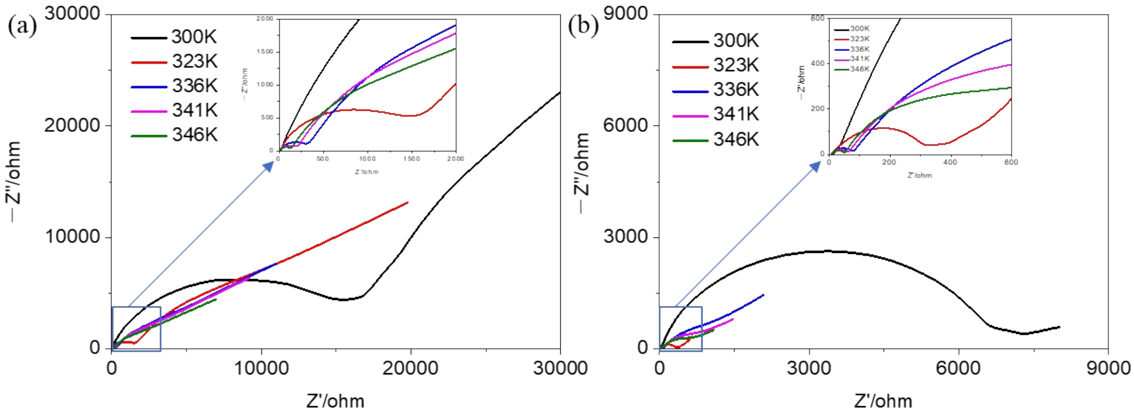

Figure S11 Nyquist plot of the cell measured at different temperatures before (a) and after (b) cycling.

3. Tables

Table S1. Elemental composition analysis by ICP-AES.

	Calcination Temperature (℃)	molar ratio	
		Na	Co
$NaCo(acac)_3$	RT	1.012(2)	1.000(2)
mixture	400	0.988(2)	1.000(2)
P3-Na_xCoO_2	600	0.788(2)	1.000(2)
P2-Na_xCoO_2	850	0.772(2)	1.000(2)

Table S2 Crystal Data and Structure Refinement Parameters for $NaCo(acac)_3$.

chemical formula	$NaCo(acac)_3$
fw	379.24
cryst size (mm^3)	0.45×0.08×0.08
T (K)	293(2)
λ (Cu, Kα, Å)	1.54187
cryst syst	Trigonal
space group	R-3c (167)
a (Å)	16.321(6)
c (Å)	11.887(11)
V (Å^3)	2742(3)
Z	6
D_{calcd} (g*cm^{-3})	1.378
μ (mm^{-1})	7.818
F(000)	1182
θ range (deg.)	4.9 – 58.7
measd. reflns	456
indep. reflns/ R_{int}	412/0.1037
obsd. reflns	412
R1^a ($I > 2\sigma(I)$)	0.1043
wR2^b (all data)	0.3295
GOF on F^2	1.037
$\Delta\rho_{max}/\Delta\rho_{min}$, e/Å^3	0.303/-0.393

^{a}R1 = $||F_o| - |F_c||/|F_o|$. ^{b}wR^2 = $[w(F_o^2 - F_c^2)^2]/[w(F_o^2)^2]^{1/2}$.

Table S3 Atomic Coordinates, Occupancies and Equivalent Isotropic Displacement Parameters for $NaCo(acac)_3$.

atom	x	y	z	U(eq)	Occupancies

Na(1)	0.666667	0.333333	0.333333	0.119(18)	1
Co(1)	0.666667	0.333333	0.083333	0.102(7)	1
O(1)	0.6230(9)	0.2144(14)	-0.0217(16)	0.076(8)	1
C(1)	0.5953(16)	0.074(2)	-0.1019(17)	0.150(15)	1
C(2)	0.666667	0.133(2)	0.083333	0.057(17)	1
C(3)	0.639(2)	0.1519(19)	0.0005(18)	0.102(15)	1

Table S4 Bond lengths (Å) and angles (°) for NaCo(acac)$_3$.

Na(1)-O(1)#1	2.42(2)	O(1)#2-Na(1)-Co(1)#7	44.6(5)
Na(1)-O(1)#2	2.42(2)	O(1)#3-Na(1)-Co(1)#7	135.4(5)
Na(1)-O(1)#3	2.42(2)	O(1)#4-Na(1)-Co(1)#7	135.4(5)
Na(1)-O(1)#4	2.42(2)	O(1)#5-Na(1)-Co(1)#7	44.6(5)
Na(1)-O(1)#5	2.42(2)	O(1)#6-Na(1)-Co(1)#7	44.6(5)
Na(1)-O(1)#6	2.42(2)	Co(1)-Na(1)-Co(1)#7	180
Na(1)-Co(1)	2.972(3)	O(1)#8-Co(1)-O(1)	88.6(8)
Na(1)-Co(1)#7	2.972(3)	O(1)#8-Co(1)-O(1)#1	102.1(8)
Co(1)-O(1)#8	2.11(2)	O(1)-Co(1)-O(1)#1	82.6(11)
Co(1)-O(1)	2.11(2)	O(1)#8-Co(1)-O(1)#3	82.6(11)
Co(1)-O(1)#1	2.11(2)	O(1)-Co(1)-O(1)#3	165.9(9)
Co(1)-O(1)#3	2.11(2)	O(1)#1-Co(1)-O(1)#3	88.6(8)
Co(1)-O(1)#4	2.11(2)	O(1)#8-Co(1)-O(1)#4	165.9(9)
Co(1)-O(1)#9	2.11(2)	O(1)-Co(1)-O(1)#4	102.1(8)
O(1)-C(3)	1.20(4)	O(1)#1-Co(1)-O(1)#4	88.6(8)
C(1)-C(3)	1.64(3)	O(1)#3-Co(1)-O(1)#4	88.6(8)

C(2)-C(3)	1.18(3)	O(1)#8-Co(1)-O(1)#9	88.6(8)
C(2)-C(3)#1	1.18(3)	O(1)-Co(1)-O(1)#9	88.6(8)
□	□	O(1)#1-Co(1)-O(1)#9	165.9(9)
O(1)#1-Na(1)-O(1)#2	105.1(7)	O(1)#3-Co(1)-O(1)#9	102.1(8)
O(1)#1-Na(1)-O(1)#3	74.9(7)	O(1)#4-Co(1)-O(1)#9	82.6(11)
O(1)#2-Na(1)-O(1)#3	105.1(7)	O(1)#8-Co(1)-Na(1)#4	53.7(5)
O(1)#1-Na(1)-O(1)#4	74.9(7)	O(1)-Co(1)-Na(1)#4	53.7(5)
O(1)#2-Na(1)-O(1)#4	180	O(1)#1-Co(1)-Na(1)#4	126.3(5)
O(1)#3-Na(1)-O(1)#4	74.9(7)	O(1)#3-Co(1)-Na(1)#4	126.3(5)
O(1)#1-Na(1)-O(1)#5	105.1(7)	O(1)#4-Co(1)-Na(1)#4	126.3(5)
O(1)#2-Na(1)-O(1)#5	74.9(7)	O(1)#9-Co(1)-Na(1)#4	53.7(5)
O(1)#3-Na(1)-O(1)#5	180	O(1)#8-Co(1)-Na(1)	126.3(5)
O(1)#4-Na(1)-O(1)#5	105.1(7)	O(1)-Co(1)-Na(1)	126.3(5)
O(1)#1-Na(1)-O(1)#6	180	O(1)#1-Co(1)-Na(1)	53.7(5)
O(1)#2-Na(1)-O(1)#6	74.9(7)	O(1)#3-Co(1)-Na(1)	53.7(5)
O(1)#3-Na(1)-O(1)#6	105.1(7)	O(1)#4-Co(1)-Na(1)	53.7(5)
O(1)#4-Na(1)-O(1)#6	105.1(7)	O(1)#9-Co(1)-Na(1)	126.3(5)
O(1)#5-Na(1)-O(1)#6	74.9(7)	Na(1)#4-Co(1)-Na(1)	180
O(1)#1-Na(1)-Co(1)	44.6(5)	C(3)-O(1)-Co(1)	122.3(17)
O(1)#2-Na(1)-Co(1)	135.4(5)	C(3)-O(1)-Na(1)#4	137.4(17)
O(1)#3-Na(1)-Co(1)	44.6(5)	Co(1)-O(1)-Na(1)#4	81.7(7)
O(1)#4-Na(1)-Co(1)	44.6(5)	C(3)-C(2)-C(3)#1	127(5)
O(1)#5-Na(1)-Co(1)	135.4(5)	C(2)-C(3)-O(1)	132(3)
O(1)#6-Na(1)-Co(1)	135.4(5)	C(2)-C(3)-C(1)	119(3)

O(1)#1-Na(1)-Co(1)#7	135.4(5)	O(1)-C(3)-C(1)	107(2)

Symmetry codes: (#1) -x+4/3,-x+y+2/3,-z+1/6; (#2) -y+1,-x+1,z+1/2; (#3) x-y+1/3,-y+2/3,-z+1/6; (#4) y+1/3,x-1/3,-z+1/6; (#5) -x+y+1,y,z+1/2; (#6) x,x-y,z+1/2; (#7) -x+4/3,-y+2/3,-z+2/3; (#8) -y+1,x-y,z; (#9) -x+y+1,-x+1,z.

Table S5. XRD Refinement parameters of NaCo(acac)$_3$ and Na$_x$CoO$_2$.

	NaCo(acac)$_3$	Na$_x$CoO$_2$
Space group	*R*-3*c*	*P*6$_3$/*mmc*
wRp	0.0592	0.0466
Rp	0.0353	0.0321
a (Å)	16.3216(26)	2.83005(34)
c (Å)	11.8897(18)	10.9142(18)
c/a	-	3.857

Table S6. EIS parameters calculated from the Nyquist plots before and after cycling in **Figure S10** for Na$_x$CoO$_2$.

Parameters	Before cycling	After cycling
R_s (Ω)	4.589	3.921
R_{ct} (Ω)	1188	260
C_d (F)	2.394E-006	8.419E-006
Activation Energy (eV/atom)	~1.04	~0.58

Table S7. The comparison of the rate capability for Na$_x$CoO$_2$ between the previous reports and this work.

	Material	Method	Rate capability (mAh g^{-1})
This work	P2-Na$_{0.77}$CoO$_2$	single-source precursor	104 at 100 mA g^{-1}; 70 at 2000 mA g^{-1}
Ref.[1]	P2- Na$_{0.67}$CoO$_2$	solid state	130 at 100 mA g^{-1}; 40 at 2000 mA g^{-1}
Ref.[2]	P2- Na$_{0.7}$CoO$_2$	solid state	112 at 100 mA g^{-1};

			64 at 2000 mA g^{-1}
Ref.[3]	P2-Na_xCoO_2	solid state	105 at 111 mA g^{-1}; 65 at 555 mA g^{-1}
Ref.[4]	P2-Na_xCoO_2	solid state	80 at 118 mA g^{-1}; 50 at 470 mA g^{-1}
Ref.[5]	P2- $Na_{0.71}CoO_2$	solid state	80 at 40 mA g^{-1}; 45 at 80 mA g^{-1}
Ref.[6]	Na_xCoO_2 (*Cmcm*）	solid state	62.3 at 80 mA g^{-1}; 28.8 at 650 mA g^{-1}

References

1. S. M. Kang, J. H. Park, A. Jin, Y. H. Jung, J. Mun and Y. E. Sung, *ACS Appl Mater Interfaces*, 2018, **10**, 3562-3570.
2. Y. J. Fang, X. Y. Yu and X. W. Lou, *Angew Chem Int Edit*, 2017, **56**, 5801-5805.
3. M. Matsui, F. Mizukoshi and N. Imanishi, *J Power Sources*, 2015, **280**, 205-209.
4. S. C. Han, H. Lim, J. Jeong, D. Ahn, W. B. Park, K. S. Sohn and M. Pyo, *J Power Sources*, 2015, **277**, 9-16.
5. M. D'Arienzo, R. Ruffo, R. Scotti, F. Morazzoni, C. M. Maria and S. Polizzi, *Phys Chem Chem Phys*, 2012, **14**, 5945-5952.
6. A. K. Rai, L. T. Anh, J. Gim, V. Mathew and J. Kim, *Ceram Int*, 2014, **40**, 2411-2417.